

Validation of Geant4 Atomic Relaxation against the NIST Physical Reference Data

S. Guatelli, A. Mantero, B. Mascialino, M. G. Pia, and V. Zampichelli

Abstract— The accuracy of the Geant4 component for the simulation of atomic relaxation has been evaluated against the experimental measurements of the NIST Standard Reference Data. The validation study concerns X-ray and Auger transition energies. The comparison of the simulated and experimental data with rigorous statistical methods demonstrates the excellent accuracy of the simulation of atomic de-excitation in Geant4.

Index Terms— Geant4, Monte Carlo, simulation, fluorescence, Auger electron.

I. INTRODUCTION

THE Low Energy Electromagnetic [1]-[2] package of the Geant4 [3]-[4] toolkit provides a precise simulation of the electromagnetic interactions of particles with matter [5]. Its modelling approach takes into account the atomic structure of matter, by describing particle interactions with the target material at the level of the atomic shells involved. A component of this package is responsible for the simulation of the atomic relaxation [6]-[7]: that is, the process following the creation of a vacancy in the shell occupancy of an atom as the result of a primary interaction process.

This paper presents a systematic, quantitative validation of the Geant4 Atomic Relaxation software component against the reference experimental data of X-ray and Auger transitions collected by the NIST (United States National Institute of Standards and Technologies) [8] in its public databases. An accurate and comprehensive validation of Geant4 physics models against authoritative reference experimental data is essential to establish the reliability of Geant4-based simulations. In the case of the Geant4 Atomic Relaxation, a quantitative estimate of its accuracy is especially important, since this software component is used in critical simulation applications, like space science missions [9]-[10] and oncological radiotherapy [11].

The simulation results presented in this paper were produced with the Low Energy Electromagnetic package publicly released in Geant4 version 8.2 and the associated data library G4EMLOW4.2. The Geant4 test process verifies that the accuracy of the Atomic Relaxation component

documented in this paper will not deteriorate in future versions of the toolkit with respect to the present results.

II. OVERVIEW OF GEANT4 ATOMIC RELAXATION SIMULATION

Some interactions, like the photoelectric effect or the ionization produced by the impact of electrons or other particles, leave the target atom in an excited state by creating an inner-shell vacancy. The relaxation of the atom can occur through the emission of X-rays or electrons. A brief summary of the Geant4 Atomic Relaxation simulation is included here; more details can be found in [7].

The simulation of the atomic relaxation proceeds through two stages in Geant4: first the shell where the vacancy is created by the primary process is sampled on the basis of the cross sections for the given physics process; then the de-excitation chain is initiated, starting from the vacancy created by the primary process: this process leads to the production of secondary photons or electrons through radiative or non-radiative transitions, the latter including Auger and Coster-Kronig transitions. The first stage is managed by the Geant4 Low Energy Electromagnetic process responsible for the primary interaction, while the second one is handled by the Geant4 Atomic Relaxation component. Non-radiative transitions are handled by Geant4 Atomic Relaxation without distinguishing proper Auger and Coster-Kronig ones; they are all referred to as “Auger” in the following paragraphs.

The generation of secondary products through the atomic relaxation mechanism is subject to the same criteria as for other Geant4 physics processes: a fluorescence photon or an Auger electron are generated as proper secondary particles, if their energy results above the production threshold defined for the region of the experimental set-up where the primary process occurs; otherwise, no secondary product is created, and the corresponding energy is converted into a local energy deposit associated to the current step of the incident particle transport. The secondary particles generated by the Atomic Relaxation are handed back to the primary processes, and by them to Geant4 tracking for further processing.

The Geant4 simulation of the atomic relaxation exploits the Evaluated Atomic Data Library (EADL) [12]; in particular, the calculation of the energy of the emitted X-ray photon or Auger electron is based on the EADL data of the binding energies of the corresponding shells involved in the transition; in this respect the Atomic Relaxation falls into the category of Geant4 “data-driven” models, while the primary processes

Manuscript received January 12, 2007.

S. Guatelli, A. Mantero, B. Mascialino, M. G. Pia, and V. Zampichelli are with INFN Sezione di Genova, 16146 Genova, Italy (telephone: +39 010 353 6328, fax: +39 010 313358, e-mail: Susanna.Guatelli@ge.infn.it, Alfonso.Mantero@ge.infn.it, Barbara.Mascialino@ge.infn.it, MariaGrazia.Pia@ge.infn.it, Valentina.Zampichelli@ge.infn.it).

that trigger it are handled by “theory-driven” or “parameterised” models. The binding energies in EADL are tabulations deriving from theoretical calculations [13]-[15] in neutral atoms.

The simulation model encompasses some approximations: the atoms are supposed to be free, and the binding energies of a neutral atom are used to compute the energy of the secondary particles emitted, thus neglecting the effects on the shell binding energies due to the fact that the atom subject to the relaxation has been ionized. These approximations are motivated by reasons of simplicity and convenience: no systematic theoretical calculations of the binding energies of a ionized atom are available in literature nor any comprehensive collections of experimental data in ionized conditions suitable to be used in a general-purpose Monte Carlo system. While these assumptions may look plausible, only a systematic validation against experimental data can confirm whether they are acceptable for Geant4 simulation applications; the validation process should also evaluate their impact quantitatively.

Geant4 Atomic Relaxation component handles elements with atomic number between 6 and 100. The atoms subject to relaxation can be pure elements or constituents of compound materials.

III. THE VALIDATION PROCESS

A. Concepts and methods

The test process of physics simulation software involves various activities: some, like unit, integration and system testing are common to any software development life-cycle, while others – like verification and validation – assume a specific connotation in the case of Monte Carlo developments for physics application.

Verification and validation are the processes of providing evidence that, respectively, the software conforms to requirements and it solves the right problem [16]. Specifically, in the case of physics simulation software [17] the verification process determines that the implementation of a physics model accurately reproduces the conceptual description of the model itself – for instance, its compliance with a theoretical formulation, while the validation process evaluates the results the simulation produces in comparison to experimental data [18].

The recent technological evolution of physics software through the adoption of the object oriented technology allows a more precise characterization of the simulation validation process by distinguishing activities with different conceptual and technical features. In fact, in the cases where the simulation software relies on a component-based architecture, one can identify two distinct aspects, which are defined in the following as “microscopic” and “macroscopic” validation respectively.

The microscopic validation concerns the comparison of the basic elements of a physics simulation model against experimental references: in a component architecture the

detailed features of a simulated process, like the energy spectra or the angular distributions of the final state products, can be validated independently. The macroscopic validation, instead, concerns the comparison of simulation results on the full scale of experimental use cases. The microscopic validation concerns a specific software component, while the macroscopic validation usually involves several components of a Monte Carlo software system and their interactions. A rigorous microscopic validation of simulation software is propaedeutical to its validation in an experimental use case; at the same time, the independent evaluation of the accuracy of simulation components allows the developers to further refine them, if necessary, and the users to estimate their contribution to the overall precision of their simulation application.

Some preliminary validation of Geant4 Atomic Relaxation has been performed both at the microscopic [6] and macroscopic [10] level; however, these tests were limited in scope, as they concerned a small number of materials irradiated and transitions observed and, in the case of experimental use cases, the complexity of the experimental set-up hindered a clear understanding of some of the effects observed. These preliminary studies motivated the need of a systematic microscopic validation of Geant4 Atomic Relaxation.

This paper documents an extensive, systematic validation study of Geant4 Atomic Relaxation against two data sets of the authoritative NIST Standard Reference Data [8]: the X-ray Transition Energies Database [19] and the Auger electron kinetic energies of the X-ray Photoelectron Spectroscopy Database [20]. The validation has been conducted with rigorous statistical analysis methods to evaluate the accuracy of the Geant4 simulation quantitatively.

A software test was specifically designed for the microscopic validation study to exercise the Geant4 Atomic Relaxation independently from other Geant4 components; this strategy ensured that the validation results could be ascribed to the component under study only, avoiding any possible interference with the physics models and software implementations of the associated primary processes, or of other Geant4 components.

B. Production of the simulation data

The simulated data were generated by means of a dedicated Geant4 application code. This test creates an excited atom by defining a vacancy in the atomic structure of a user-selected target material, and hands it to the interface object of the Atomic Relaxation package, which steers the de-excitation process. The public interface of the objects representing the secondary products of the atomic de-excitation allows retrieving the physical information relevant to the validation study: the energy and type (photon or electron) of the particles generated, and the identification of the shells involved in each transition. The significant physics quantities associated to each transition are encapsulated in AIDA [21] objects for further analysis. PI [22] was used as a concrete AIDA implementation in the simulation production.

The simulation test was executed for all the elements handled by Geant4 Atomic Relaxation component, i.e. with atomic number between 6 and 100. The test management ensured that all the radiative and non-radiative transitions modelled in Geant4 were produced at least once in the simulation irrespective of their associated occurrence probability; therefore the sample of simulated secondary photons and Auger electrons subject to validation represents the Geant4 transition energy spectra exhaustively.

C. Reference experimental data

The NIST Reference Data collection includes two databases relevant to atomic relaxation processes: the X-ray Transition Energies [19] and the X-ray Photoelectron Spectroscopy Database [20], concerning atomic radiative and non-radiative transitions respectively.

The NIST X-ray Transition Energies database derives from a thorough review [23] of the body of knowledge concerning X-ray transitions; the available data were subject to an evaluation procedure and to appropriate corrections. The compilation includes both experimental measurements and theoretical calculations; only the subset corresponding to experimental data was considered for Geant4 validation purposes. The reference data concern K and L X-ray transitions for elements with atomic number between 10 (Neon) and 100 (Fermium): transitions connecting the K shell to the shells with principal quantum numbers 2 to 4, and transitions connecting the L_1 , L_2 , and L_3 shells to the shells with principal quantum numbers 3 and 4. The reported values have been corrected for all known errors and are determined using appropriate units conversion factors. The uncertainties of the experimental data are reported in [23]. The 10-100 range of atomic numbers mentioned above refers to the comprehensive coverage of theoretical and experimental data reported in the review; the experimental transitions listed in [23] cover various subsets of this range depending on the type of transition.

The NIST X-ray Photoelectron Spectroscopy (XPS) Database collects the energies of many photoelectron and Auger-electron spectral lines measured experimentally. It results from a critical evaluation of the published literature; while the NIST values of the X-ray transition energies result from a coherent evaluation and correction procedure, this database appears to be organized as a collection of references to independent measurements. Many entries of the database indicate that the related transition is unresolved; for many transitions the database lists multiple associated measurements rather than a unique evaluated value. The uncertainties of the experimental data are reported in the individual references listed in the XPS database for each transition energy measurement.

All the reference data were automatically downloaded from the NIST web site through a Python [24] script and encapsulated in AIDA analysis objects by means of PI Python binding.

D. Data analysis

The data analysis consisted of the comparison of simulated and experimental data samples of secondary particle energies produced by X-ray and Auger transitions respectively. The analysis procedure was similar in the two cases, and included two phases: the selection of the data samples to be subject to the comparison, and a statistical estimation of their compatibility through goodness-of-fit tests.

From a physics perspective, the analysis addressed various complementary aspects: the overall evaluation of the Geant4 simulation accuracy, a detailed characterization of the simulation accuracy according to the type of transition involved and the atomic number of the target element, and the study of possible systematic effects introduced in the analysis itself.

1) Selection of the data samples

The first step of the data selection consisted of the identification of the simulated and reference samples corresponding to the same transitions in the AIDA objects produced by the simulation.

Geant4 Atomic Relaxation component is capable to generate atomic transitions concerning the sub-shells of K, L, M, N shells and some O sub-shells; some of these transitions are not envisaged in the NIST reference databases, and could not be subject to the validation process described in this paper for obvious reasons. The design of the Geant4 Atomic Relaxation allows retrieving detailed information about the transition characteristics, such as the identification of the participating sub-shells.

This preliminary sample selection process was easily performed in the case of X-ray transitions, since in most cases the NIST database identifies the sub-shells involved in each transition energy entry; the XPS database, instead, reports most transitions as unresolved at the sub-shell level, but only identified in terms of the participating shells. In the case when the transition type could not be unambiguously resolved in the NIST reference data set, all the transition energies corresponding to possible associated sub-shells were included in the simulated data sample. The data samples selected at this stage were suitable for a statistical analysis of the overall accuracy of Geant4 X-ray and Auger transition energies.

The simulated and reference data were further grouped according to the initial sub-shell vacancy for more detailed comparison analysis. In the case of X-ray transitions the abundance of reference data allowed further grouping the samples in terms of both sub-shells involved.

2) Statistical analysis

The agreement between the simulated and the experimental data set was evaluated quantitatively by means of a goodness-of-fit test. Two hypotheses were formulated to define the test in statistical terms: the null hypothesis stated the equivalence between reference data and Geant4 simulations for all the elements considered; the alternative hypothesis stated that the two sets of data differed.

The result of a goodness-of-fit test is expressed numerically by a p-value, which represents the probability that the test

statistic has a value at least as extreme as that observed, assuming that the null hypothesis is true. In the statistical analysis practice it is customary to set confidence levels to define the success of a goodness-of-fit test: p-values greater than the selected confidence level lead to the acceptance of the null hypothesis, i.e. establish the compatibility of the two data samples under test. Typical confidence level settings are 0.01, 0.05 and 0.1, the higher values expressing stricter requirements for the compatibility of the two data sets.

The Statistical Toolkit [25]-[26] was used for the statistical analysis through its user layer component interfaced to AIDA. The rich collection of goodness-of-fit tests offered by this software system allows applying different algorithms to the same data samples to evaluate the sensitivity of the final result to the choice of the comparison method, thus identifying the possible introduction of systematic effects in the data analysis.

The Kolmogorov-Smirnov test [27]-[28] was applied to all the comparisons documented in the following section, as it is appropriate to the characteristics of all the distributions considered [29]. Other goodness-of-fit tests were used in selected cases to evaluate possible systematic effects affecting the validation results.

IV. RESULTS

The different characteristics of the two NIST databases affect the validation analysis process and results. The comparison analysis of the X-ray transition energies profits of some specific features of the reference data sample: the univocal association between one value for each transition considered in the NIST database and a corresponding simulated one, the unambiguous identification of the shell involved in most transitions, and, more in general, the coherence of the compilation resulting from the evaluation procedure documented in [23]. These considerations should be taken into account when appraising the outcome of the statistical data analysis for X-ray and Auger transition energy validation respectively.

A. X-ray transitions

The X-ray energies of a few selected K and L shell transitions are plotted in Fig. 1 to Fig. 4 as a function of the atomic number Z ; they are representative of the whole collection of results. The figures show both the results generated by Geant4 Atomic Relaxation and the NIST reference values, and demonstrate the qualitative good agreement of the simulation with experimental measurements. Geant4 is capable to produce a larger set of X-ray transitions than the series reported in the NIST database; the results reported in this section concern the subset of transitions having a counterpart in the NIST database. A detailed appraisal of the accuracy of the simulated X-ray energies is shown in Fig. 5 to Fig. 8. These plots show the relative differences between simulated and experimental photon energies $(E_{\text{simulated}} - E_{\text{experimental}})/E_{\text{experimental}}$ as a function of the atomic number Z for all K and L transitions considered in this study; the values are expressed as percentage of the reference

experimental energies. The differences are smaller than 0.5% in most cases; larger differences may be related to either a degraded simulation accuracy or to poor experimental measurements; a detailed discussion of the experimental uncertainties can be found in [23], while the degradation of the simulation accuracy could be due either to a worse precision of the theoretical calculations of binding energies or to the inadequacy of the simulation modeling assumptions (such as the equivalence of the binding energies of neutral and ionized atoms).

The simulated and experimental energy distributions were subject to a rigorous statistical analysis to evaluate the accuracy of Geant4 Atomic Relaxation quantitatively. The analysis of the X-ray transition energies encompassed a global comparison of all common entries in the simulated and experimental data samples, a detailed comparison of the photon energies for each type of transition identified in the NIST database, and a comparison articulated over different ranges of the atomic number.

The global comparison of the Geant4 simulated photon energies against all NIST database entries results in a p-value of 1 from the Kolmogorov-Smirnov test. Other goodness-of-fit tests provide the same result; they are summarized in Table I. The consistency of the results of independent goodness-of-fit tests, which are based on different comparison criteria and mathematical formulations of the test statistic, exclude that the outstanding agreement between the simulated and reference data samples might be due to a mathematical artifact.

The X-ray transition data were grouped according to the shell corresponding to the initial vacancy for a more detailed analysis, and further classified according to the sub-shells involved; the resulting simulated and experimental distributions were subject to goodness-of-fit tests. The p-values obtained from the Kolmogorov-Smirnov test are listed in Table II for all the transitions associated to a vacancy in the K shell and the L_1 , L_2 and L_3 sub-shells reported in the NIST database.

All the results of the statistical analysis consistently confirm the excellent agreement between the simulated and experimental data sets.

TABLE I
GLOBAL STATISTICAL COMPARISON OF RADIATIVE TRANSITION DATA

Goodness-of-fit test	p-value
Anderson-Darling	1
Cramer-von Mises	1
Kolmogorov-Smirnov	1
Kuiper	1
Watson	1

TABLE II
RESULTS OF THE GOODNESS-OF-FIT TEST FOR SELECTED X-RAY TRANSITIONS

Transition	Kolmogorov-Smirnov test statistic	p-value
KL ₂	0.0188	1
KL ₃	0.0185	1
KM ₂	0.0172	1
KM ₄	0.0667	1
KM ₅	0.0588	1
KN ₂	0.0714	1
KN ₃	0.0714	1
L ₁ M ₂	0.0192	1
L ₁ M ₃	0.0175	1
L ₁ M ₄	0.0250	1
L ₁ M ₅	0.0256	1
L ₁ N ₂	0.0294	1
L ₁ N ₃	0.0312	1
L ₁ N ₄	0.1429	0.997
L ₁ N ₅	0.0588	1
L ₂ M ₁	0.0147	1
L ₂ M ₃	0.0435	1
L ₂ M ₄	0.0139	1
L ₂ N ₂ or L ₂ N ₃	0.0204	1
L ₂ N ₃	0.0526	1
L ₂ N ₄	0.0196	1
L ₂ N ₆	0.0714	1
L ₃ M ₁	0.0145	1
L ₃ M ₂	0.0588	1
L ₃ M ₃	0.0556	1
L ₃ M ₄	0.0181	1
L ₃ M ₅	0.0179	1
L ₃ N ₂ or L ₃ N ₃	0.0200	1
L ₃ N ₂	0.0667	1
L ₃ N ₃	0.0556	1
L ₃ N ₄	0.0588	1
L ₃ N ₅	0.0500	1

B. Auger transitions

The Auger electron energies resulting from K, L₂, L₃, M₄ and M₅ transitions are plotted in Fig. 9 and Fig. 10; the plots highlight the scarcity of NIST reference data with respect to the abundance of transitions simulated by Geant4 Atomic Relaxation. The qualitative agreement between the simulated and the available experimental data looks anyway good.

The statistical analysis of the Auger electron transitions was necessarily less articulated than the one of the X-ray ones, because of the limited number of reference data in the NIST database.

A global comparison was performed on the whole Geant4 simulated and NIST reference data samples; similarly to the case of radiative transitions, possible systematic effects due to the analysis method were studied through the application of different goodness-of-fit tests. The resulting p-values are listed in Table III: all the tests lead to the acceptance of the null hypothesis even under strict confidence level settings (p-value>0.1), and confirm the compatibility of the simulated and reference distributions as a conclusion of the validation study.

The data were grouped in terms of the sub-shell

corresponding to the initial vacancy for a further, more detailed analysis; the simulated and experimental transition energy distributions were subject to the Kolmogorov-Smirnov goodness-of-fit test. The results of the statistical analysis are summarized in Table IV: they confirm the good agreement between Geant4 simulated and reference data also at the level of each individual transition type considered.

A similar analysis was performed on the subset of ‘‘Auger principal lines’’ reported in the XPS database; the results are documented in Table V.

All the results of the statistical analysis are consistent to demonstrate the accuracy of the Geant4 simulation of Auger electron energies.

A detailed appraisal of the simulation accuracy is not practically feasible for Auger transitions: in fact, the XPS database often reports multiple measured values for a given transition, and in most cases it does not resolve the sub-shells involved in the transition. For these reasons the detailed relative differences between simulated and experimental electron energies $(E_{\text{simulated}} - E_{\text{experimental}})/E_{\text{experimental}}$ have been calculated only for the subset of the XPS database identified as ‘‘Auger principal lines’’; for these values it is possible to find a univocal association to a corresponding Geant4 transition energy; this sample spans a wide range of atomic numbers and can be considered representative of the accuracy of individual transition energies. The results are plotted in Fig. 11 as a function of the atomic number Z; the values are expressed as percentage of the reference experimental energies. The differences are smaller than 0.5% in all cases, except for the N₅N₆₇N₆₇ transition of W (Z=74), where N₅ is the subshell where the original vacancy is created, N₆₇ means N₆ or N₇ unresolved subshells and represents the shell participating in the Auger transition and the shell from which the Auger electron is ejected. It is worthwhile noticing that the relatively larger difference (approximately 3%) noticed in this case corresponds to the only N transition in the data set and a low energy measured value of 166.2 eV; the delicate condition may be problematic both for the experimental and the simulation accuracy.

TABLE III
GLOBAL STATISTICAL COMPARISON OF AUGER TRANSITION DATA

Goodness-of-fit test	p-value
Anderson-Darling	0.633
Cramer-von Mises	0.521
Kolmogorov-Smirnov	0.432
Kuiper	0.262
Watson	0.307

TABLE IV
RESULTS OF THE GOODNESS-OF-FIT TEST FOR SELECTED AUGER TRANSITIONS

Transition	Kolmogorov-Smirnov test statistic	p-value
K	0.314	0.644
L ₂	0.329	0.671
L ₃	0.162	0.628
M ₄	0.143	0.809
M ₅	0.157	0.654

TABLE V
STATISTICAL COMPARISON OF AUGER PRINCIPAL LINES

Goodness-of-fit test	p-value
Anderson-Darling	0.9999
Cramer-von Mises	0.9998
Kolmogorov-Smirnov	1
Kuiper	1
Watson	0.9993

V. CONCLUSION

A comprehensive validation study has been performed to evaluate the accuracy of the Geant4 simulation of X-ray and Auger electron energies. The results of Geant4 Atomic Relaxation component of the Low Energy Electromagnetic package have been compared to the experimental measurements of the NIST Physics Reference Data collections; the compatibility of the simulated and experimental distributions has been estimated through rigorous goodness-of-fit tests.

The results highlight the high precision of the simulation of X-ray fluorescence and Auger electron emission in the Geant4 Low Energy Electromagnetic package. This study provides a comprehensive reference to the wide Geant4 user community to evaluate the precision of the generation of atomic relaxation products in a Geant4-based simulation application.

Further validation studies of the Geant4 Atomic Relaxation component are planned, in particular concerning the transition probabilities not covered in this paper (nor in the NIST reference databases considered). Validation tests in concrete experimental use cases are in progress to demonstrate Geant4 capabilities for the simulation of X-ray fluorescence emission from complex compound materials [10]; the detailed results will be documented in a dedicated paper.

This work is part of a wider project in progress for the systematic validation of Geant4 electromagnetic physics models, with the purpose to document quantitatively the simulation accuracy achievable in Geant4 experimental applications.

VI. REFERENCES

- [1] S. Chauvie et al., "Geant4 Low Energy Electromagnetic Physics", Proc. of Computing In High Energy Physics, Beijing, 2001.
- [2] S. Chauvie et al., "Geant4 Low Energy Electromagnetic Physics", *Conf. Rec. 2004 IEEE Nucl. Sci. Symp.* Vol. 3, pp. 1881–1885, Oct. 2004.
- [3] S. Agostinelli et al., "Geant4 - a Simulation Toolkit", *Nucl. Instrum. Methods A*, vol. 506 pp. 250-303, Jul. 2003.
- [4] J. Allison, K. Amako, J. Apostolakis, H. Araujo, P. Arce Dubois, M. Asai, et al., "Geant4 developments and applications", *IEEE Trans. Nucl. Sci.*, vol. 53, no. 1, pp. 270-278, Feb. 2006.
- [5] K. Amako et al., Comparison of Geant4 electromagnetic physics models against the NIST reference data, *IEEE Trans. Nucl. Sci.*, vol. 52, no. 4, pp. 910-918, Aug. 2005.
- [6] S. Guatelli, A. Mantero, B. Mascialino, P. Nieminen, M. G. Pia, and S. Saliceti, "Geant4 Atomic Relaxation", in *Conf. Rec. 2004 IEEE Nucl. Sci. Symp.*, Oct. 2004.
- [7] S. Guatelli, A. Mantero, B. Mascialino, P. Nieminen, and M. G. Pia, "Geant4 Atomic Relaxation", submitted to *IEEE Trans. Nucl. Sci.*, Jan. 2007.
- [8] NIST Standard Reference Data [Online]. Available: <http://physics.nist.gov/srd>.
- [9] A. Owens et al., "HERMES: an imaging X-ray fluorescence spectrometer for the BepiColombo mission to Mercury", in *Proc. of SPIE - Soft X-Ray and EUV Imaging Systems II*, vol. 4506, pp. 136-145, Dec. 2001.
- [10] A. Mantero et al., "Simulation of X-ray fluorescence and application to planetary astrophysics", in *Conf. Rec. 2003 IEEE Nucl. Sci. Symp.*, Oct. 2003.
- [11] R. Taschereau, R. Roy, and J. Pouliot, "Relative biological effectiveness enhancement of a ^{125}I brachytherapy seed with characteristic X-rays from its constitutive materials", *Med. Phys.*, vol. 29, no. 7, pp. 1397-1402, 2002.
- [12] S. T. Perkins et al., Tables and Graphs of Atomic Subshell and Relaxation Data Derived from the LLNL Evaluated Atomic Data Library (EADL), Z=1-100, UCRL-50400 Vol. 30, 1997.
- [13] J. H. Scofield, "Radiative decay rates of vacancies in K and L shells", *Phys. Rev.* 179, no. 1, pp. 9-16, 1969.
- [14] J. H. Scofield, "Hartree-Fock values of L X-ray emission energies", *Phys. Rev. A* 10, pp. 1507-1510, 1974.
- [15] J. H. Scofield, "Relativistic Hartree-Slater values for K and L X-ray emission rates", *At. Data Nucl. Data Tables* 14, pp. 121-137, 1974.
- [16] IEEE Computer Society, "IEEE Standard for Software Verification and Validation", IEEE Std 1012™-2004, Jun. 2005.
- [17] T. G. Trucano, L. P. Swiler, T. Igusa, W. L. Oberkampf, and M. Pilch, "Calibration, validation, and sensitivity analysis: What's what", *Reliability Eng. and Sys. Safety*, vol. 91, pp. 1331–1357, 2006.
- [18] W. L. Oberkampf, T. G. Trucano, and C. Hirsch, "Verification, Validation, and Predictive Capability in Computational Engineering and Physics", SAND2003-3769, Feb. 2003.
- [19] NIST X-ray Transition Energies [Online]. Available: <http://physics.nist.gov/PhysRefData/XrayTrans/index.html>.
- [20] NIST X-ray Photoelectron Spectroscopy Database [Online]. Available: <http://srddata.nist.gov/xps/index.htm>.
- [21] G. Barrand, P. Binko, M. Donszelmann, A. Johnson, and A. Pfeiffer, "Abstract interfaces for data analysis: component architecture for data analysis tools", Proc. of CHEP 2001 Int. Conf. on Computing in High Energy and Nuclear Physics, pp. 215-218, Science Press, Beijing, 2001.
- [22] A. Pfeiffer, L. Moneta, V. Innocente, H. C. Lee, and W. L. Ueng, "The LCG PI project: using interfaces for physics data analysis", *IEEE Trans. Nucl. Sci.*, vol. 52, no. 6, pp. 2823 – 2826, Dec. 2005.
- [23] R. D. Deslattes, E. G. Kessler Jr., P. Indelicato, L. de Billy, E. Lindroth, and J. Anton, "X-ray transition energies: new approach to a comprehensive evaluation", *Rev. Mod. Phys.*, vol. 75, pp. 35-99, Jan. 2003.
- [24] G. van Rossum and F. L. Drake Jr., The Python Language Reference Manual, Network Theory Ltd., 2003.
- [25] G. A. P. Cirrone et al., "A Goodness-of-Fit Statistical Toolkit", *IEEE Trans. Nucl. Sci.*, vol. 51, no. 5, pp. 2056-2063, Oct. 2004.
- [26] B. Mascialino, A. Pfeiffer, M. G. Pia, A. Ribon, and P. Viarengo, "New developments of the Goodness-of-Fit Statistical Toolkit", *IEEE Trans. Nucl. Sci.*, vol. 53, no. 6, pp. 3834-3841, Dec. 2006.
- [27] N. V. Smirnov, "Sur les écarts de la courbe de distribution empirique" *Matematicheskii Sbornik N.S.*, vol. 6, pp. 3–26, 1939.
- [28] N. V. Smirnov, "Table for estimating the goodness-of-fit of empirical distributions," *Ann. Math. Statist.*, vol. 19, pp. 279–281, 1948.
- [29] S. Guatelli, B. Mascialino, A. Pfeiffer, M. G. Pia, A. Ribon, and P. Viarengo, "Application of statistical methods for the comparison of data distributions", in *Conf. Rec. 2004 IEEE Nucl. Sci. Symp.*, vol. 4, pp. 2086 – 2090, Oct. 2004.

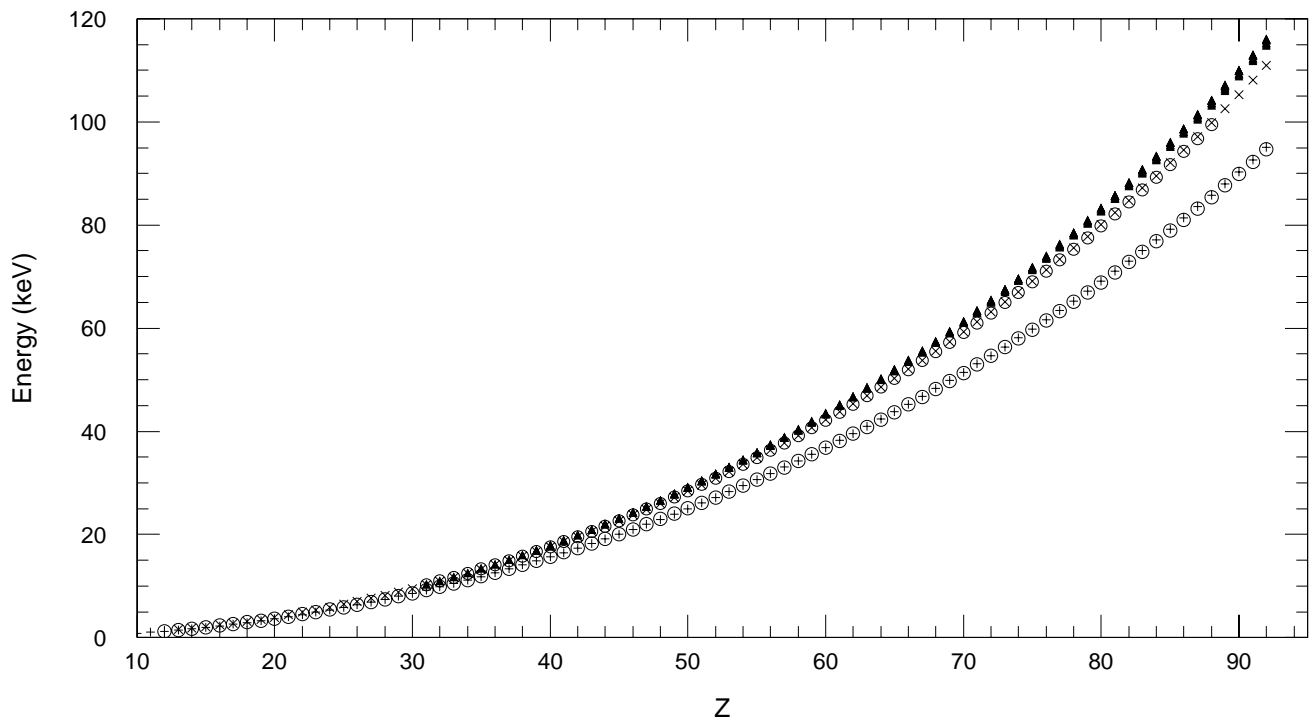


Fig. 1. A sample of K-shell X-ray transition energies as a function of the atomic number Z ; the symbols represent respectively: Geant4 KL_2 (“+”) and KM_2 (“x”) transitions and reference experimental data (circles) corresponding to the same transitions; the black symbols are Geant4 simulation results; the plot also shows K-shell transitions that Geant4 can produce (triangles), but that are not considered in the NIST reference database.

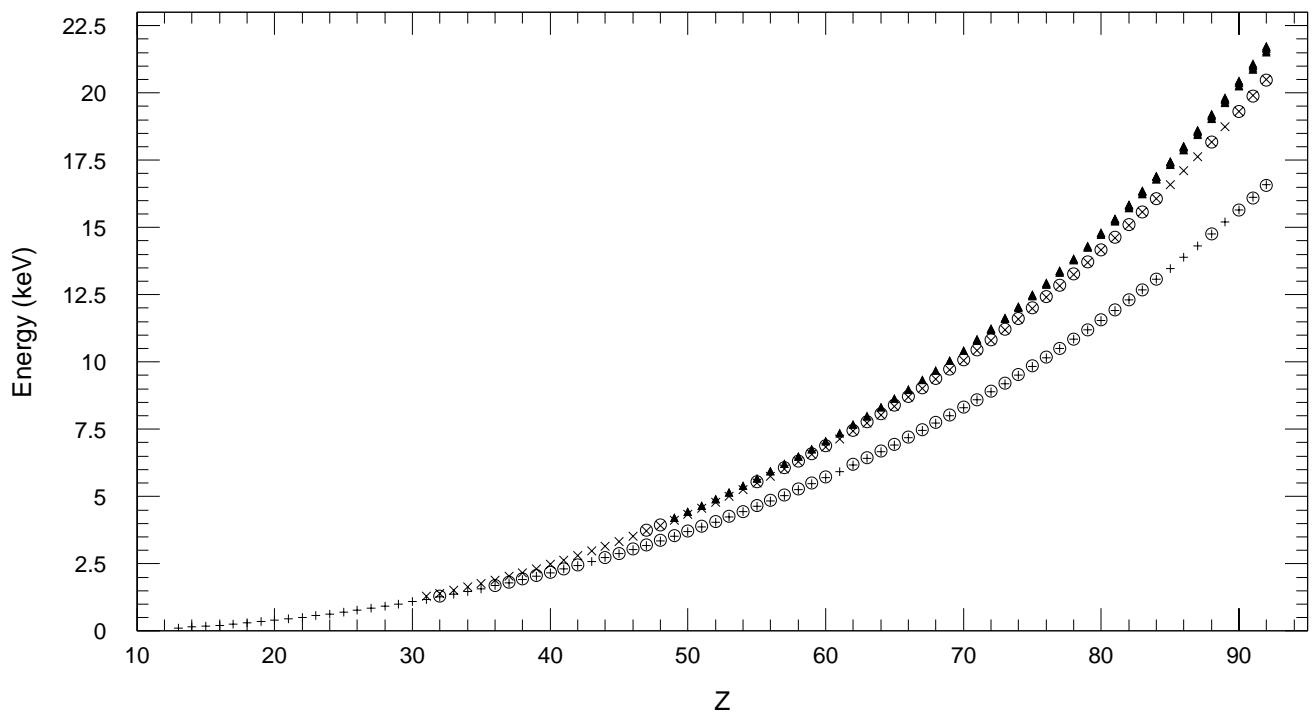


Fig. 2. A sample of L_1 X-ray transition energies as a function of the atomic number Z ; the symbols represent respectively: Geant4 L_1M_2 (“+”) and L_1N_2 (“x”) transitions and reference experimental data (circles) corresponding to the same transitions; the black symbols are Geant4 simulation results; the plot also shows L_1 -shell transitions that Geant4 can produce (triangles), but that are not considered in the NIST reference database.

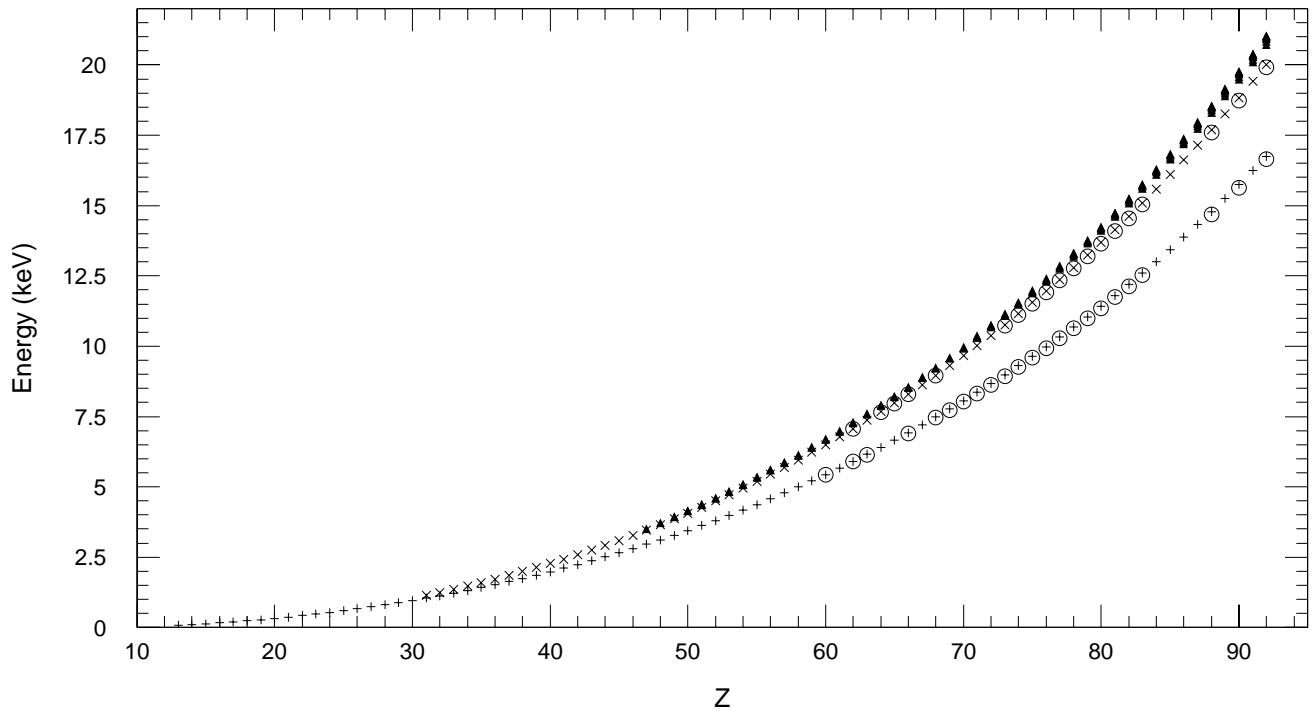


Fig. 3. A sample of L₂ X-ray transition energies as a function of the atomic number Z; the symbols represent respectively: Geant4 L₂M₃ (“+”) and L₂N₃ (“x”) transitions and reference experimental data (circles) corresponding to the same transitions; the black symbols are Geant4 simulation results; the plot also shows L₂-shell transitions that Geant4 can produce (triangles), but that are not considered in the NIST reference database.

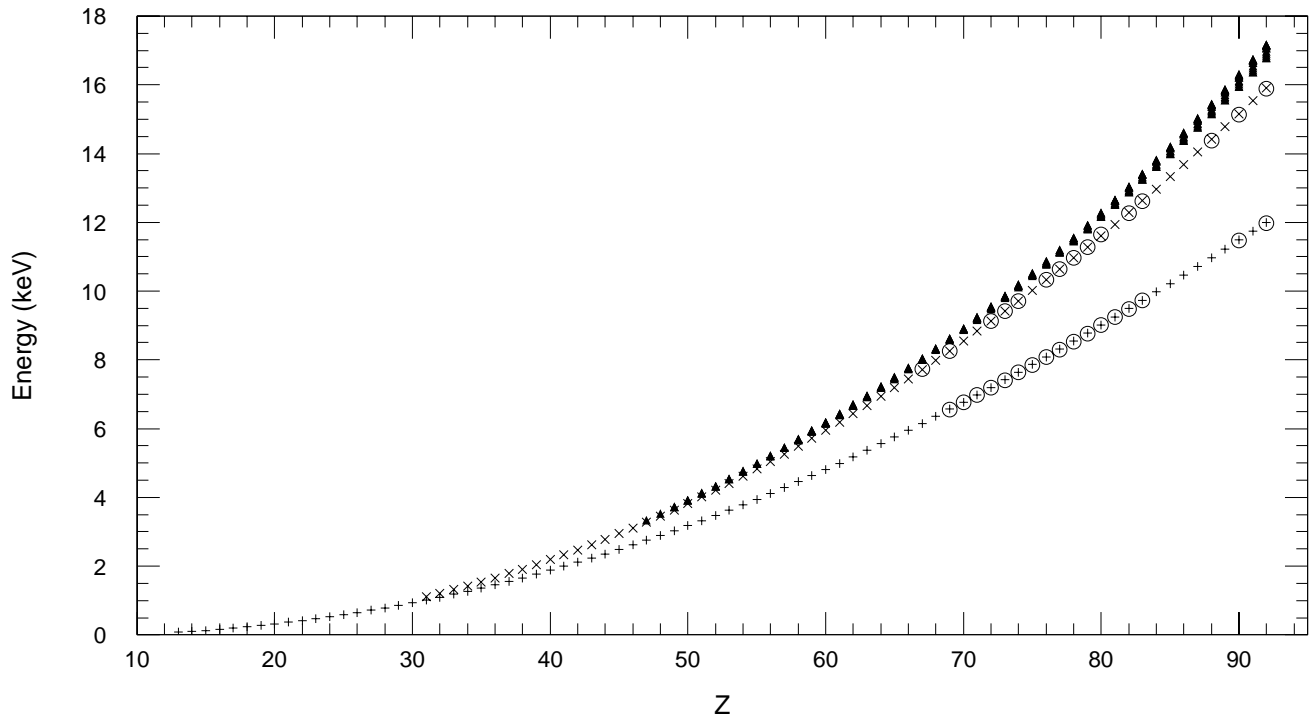


Fig. 4. A sample of L₃ X-ray transition energies as a function of the atomic number Z; the symbols represent respectively: Geant4 L₃M₂ (“+”) and L₃N₂ (“x”) transitions and reference experimental data (circles) corresponding to the same transitions; the black symbols are Geant4 simulation results; the plot also shows L₃-shell transitions that Geant4 can produce (triangles), but that are not considered in the NIST reference database.

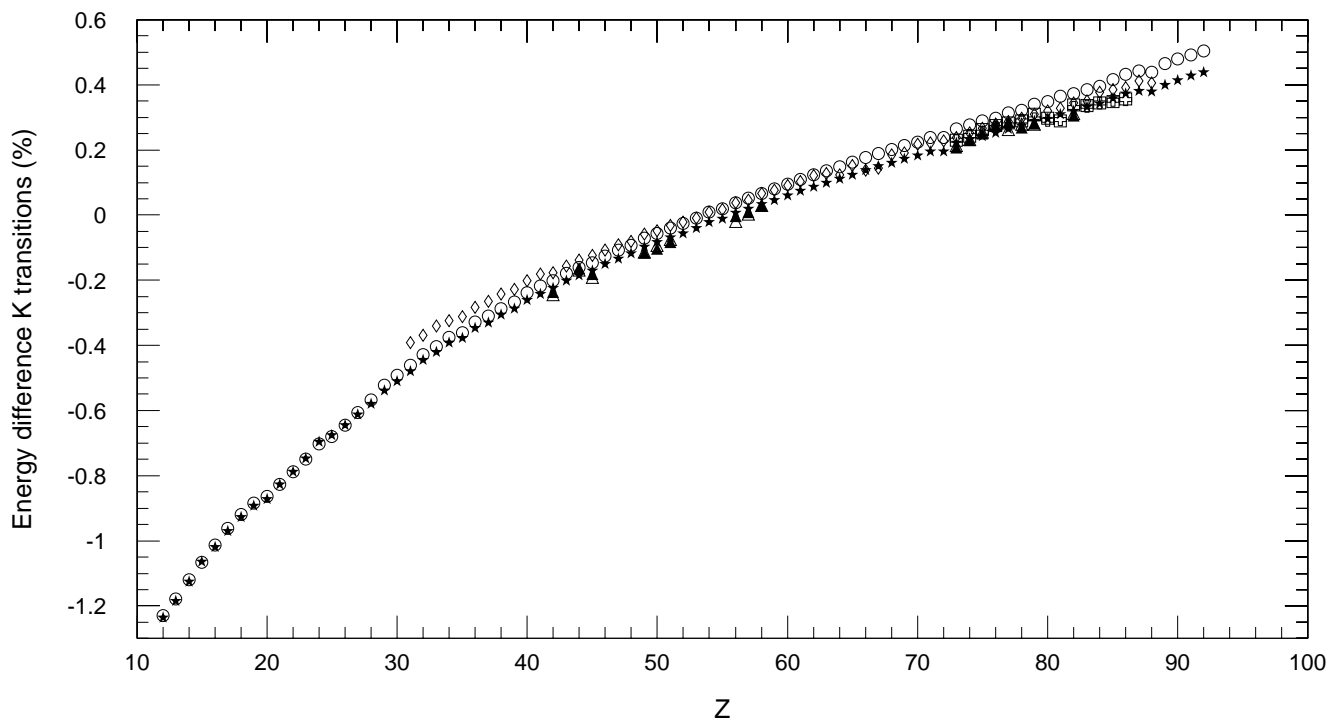


Fig. 5. Difference between Geant4-simulated and NIST reference K-shell X-ray transition energies as a function of the atomic number Z , expressed in percentage with respect to the NIST values; the symbols represent transitions concerning L_2 (stars), L_3 (circles), M_2 (diamonds), M_4 (black triangles), M_5 (white triangles), N_2 (squares) and N_3 (crosses) shells.

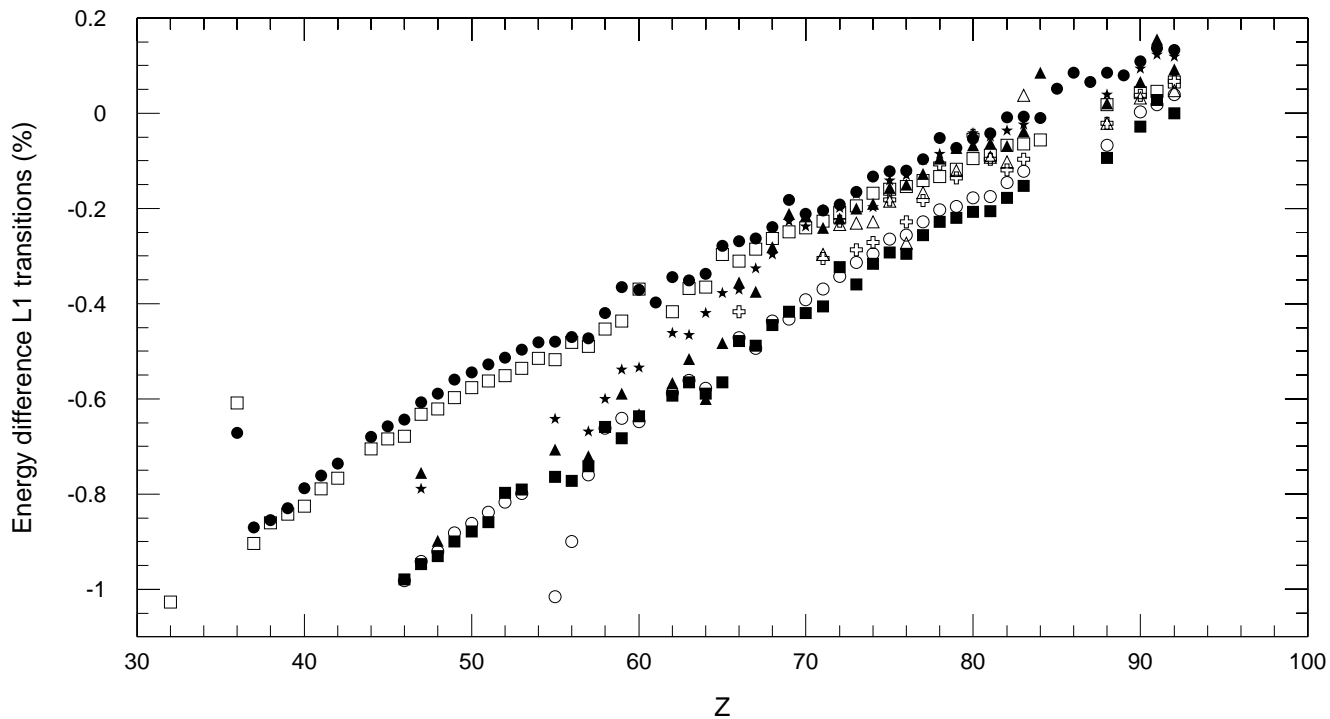


Fig. 6. Difference between Geant4-simulated and NIST reference L₁-shell X-ray transition energies as a function of the atomic number Z , expressed in percentage with respect to the NIST values; the symbols represent transitions concerning M_2 (white squares), M_3 (black circles), M_4 (black squares), M_5 (white circles), N_2 (black triangles), N_3 (stars), N_4 (white triangles) and N_5 (white crosses) shells.

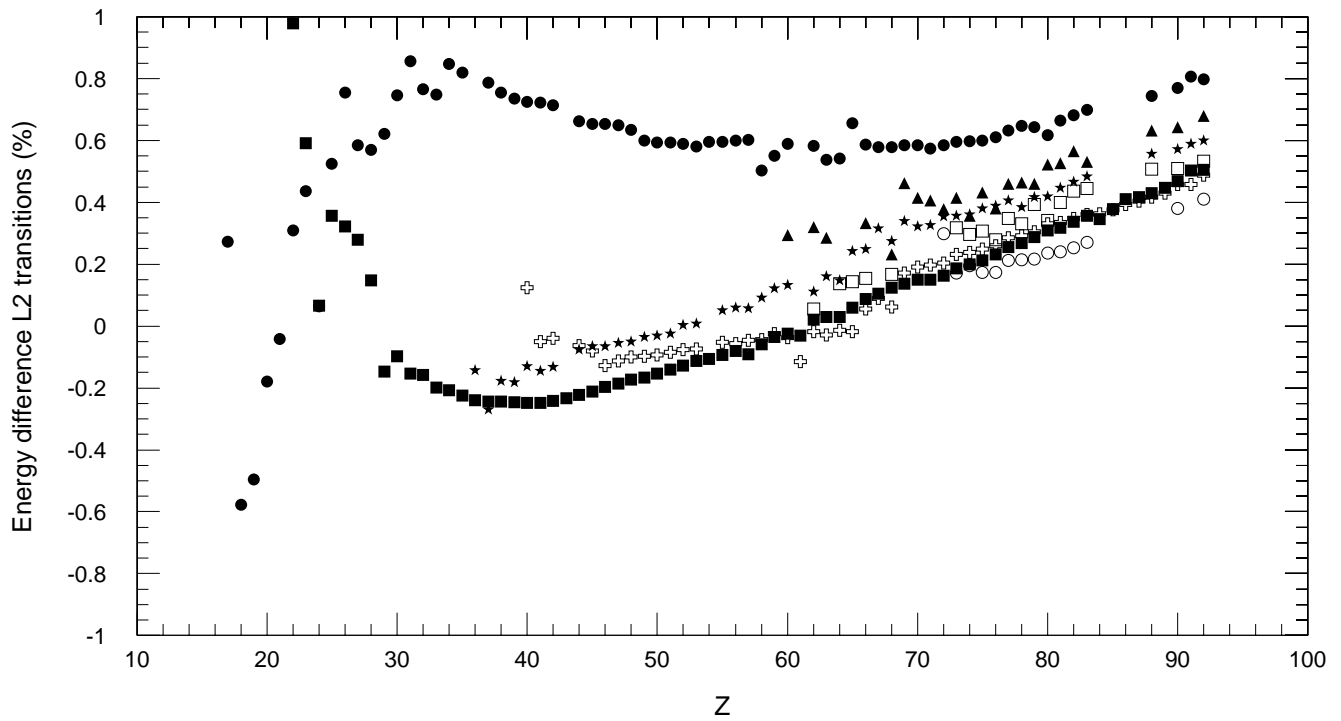


Fig. 7. Difference between Geant4-simulated and NIST reference L_2 -shell X-ray transition energies as a function of the atomic number Z , expressed in percentage with respect to the NIST values; the symbols represent transitions concerning M_1 (black circles), M_3 (black triangles), M_4 (black squares), N_2 (stars), N_5 (white squares), N_4 (white crosses) and N_6 (white circles) shells.

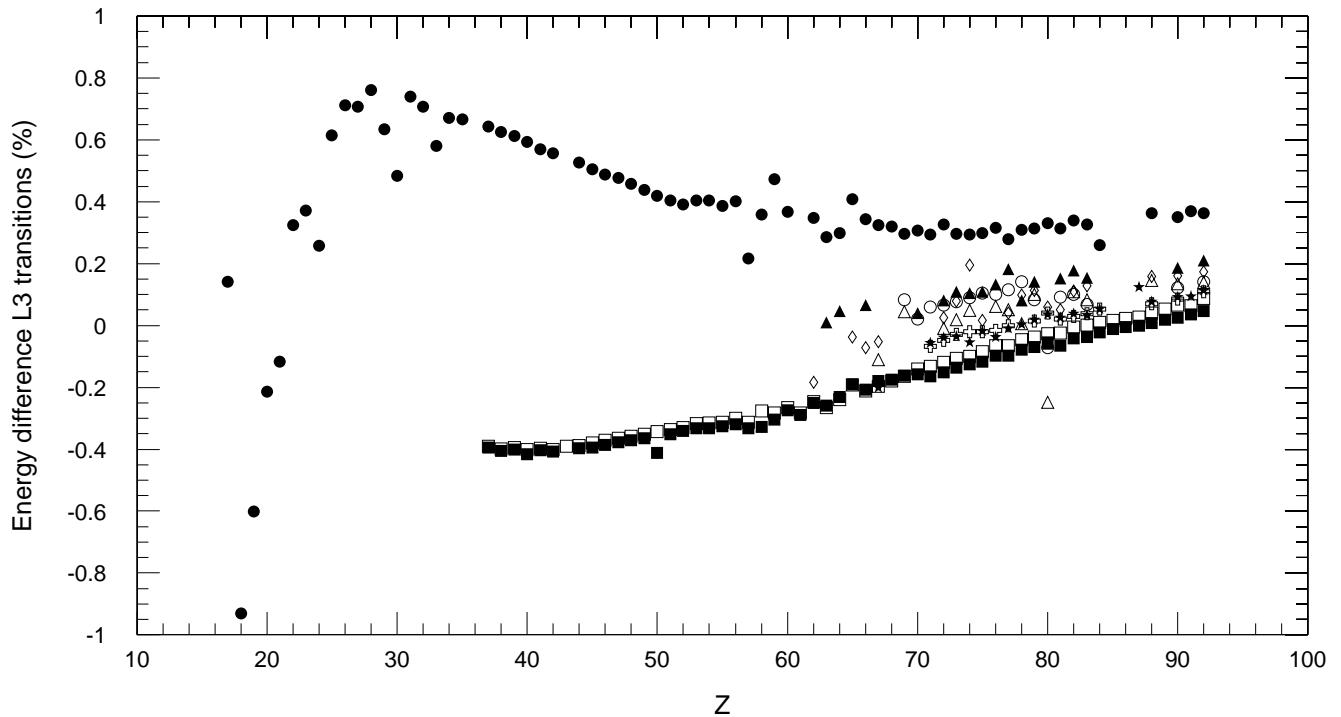


Fig. 8. Difference between Geant4-simulated and NIST reference L_3 -shell X-ray transition energies as a function of the atomic number Z , expressed in percentage with respect to the NIST values; the symbols represent transitions concerning M_1 (black circles), M_2 (white circles), M_3 (black triangles), M_4 (black squares), M_5 (white squares), N_2 (white triangles), N_3 (diamonds), N_4 (white crosses), and N_5 (stars) shells.

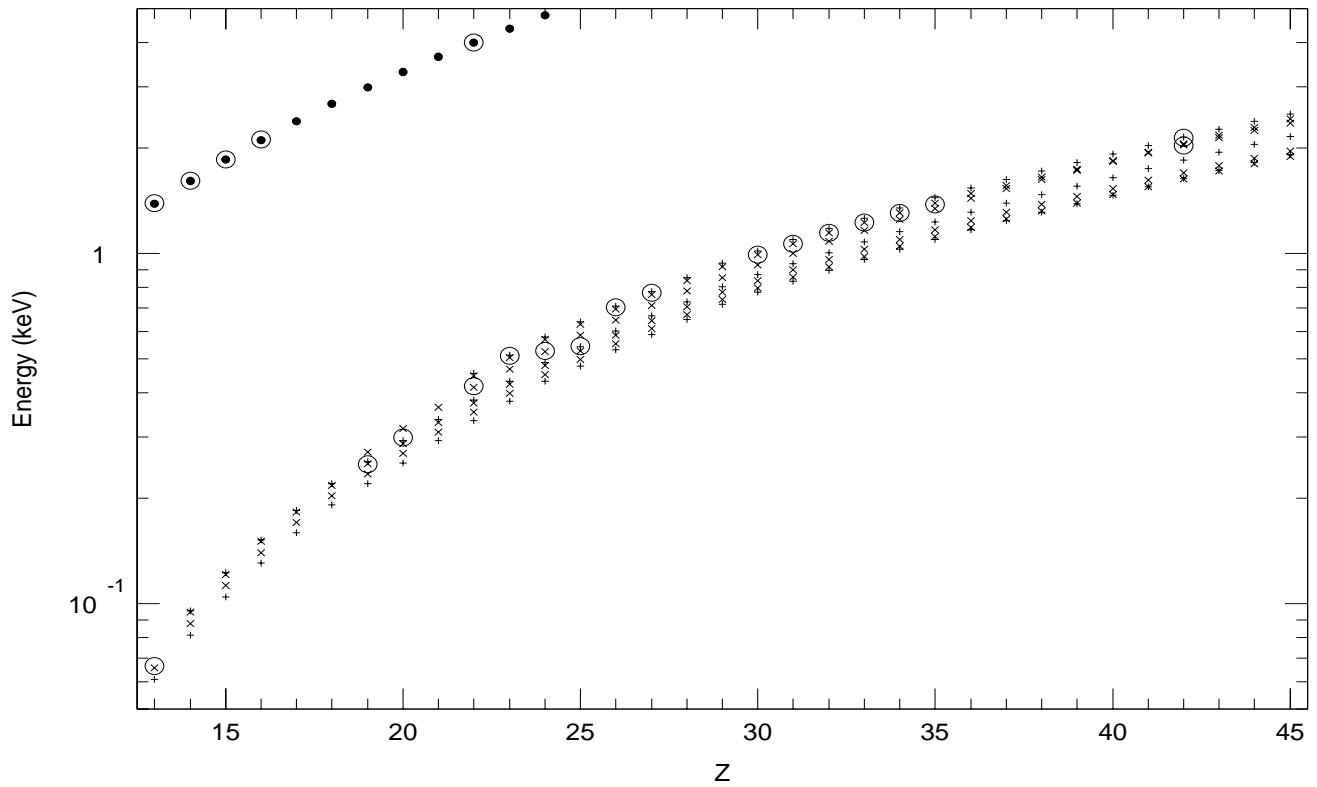


Fig. 9. Auger electron energies resulting from Geant4 K (black dots), L₂ (“+”) and L₃ (“x”) transitions and NIST reference experimental data (open circles); to improve the readability of the plot the symbols representing NIST data are scaled by a factor 2 in size with respect to the symbols representing Geant4 simulation.

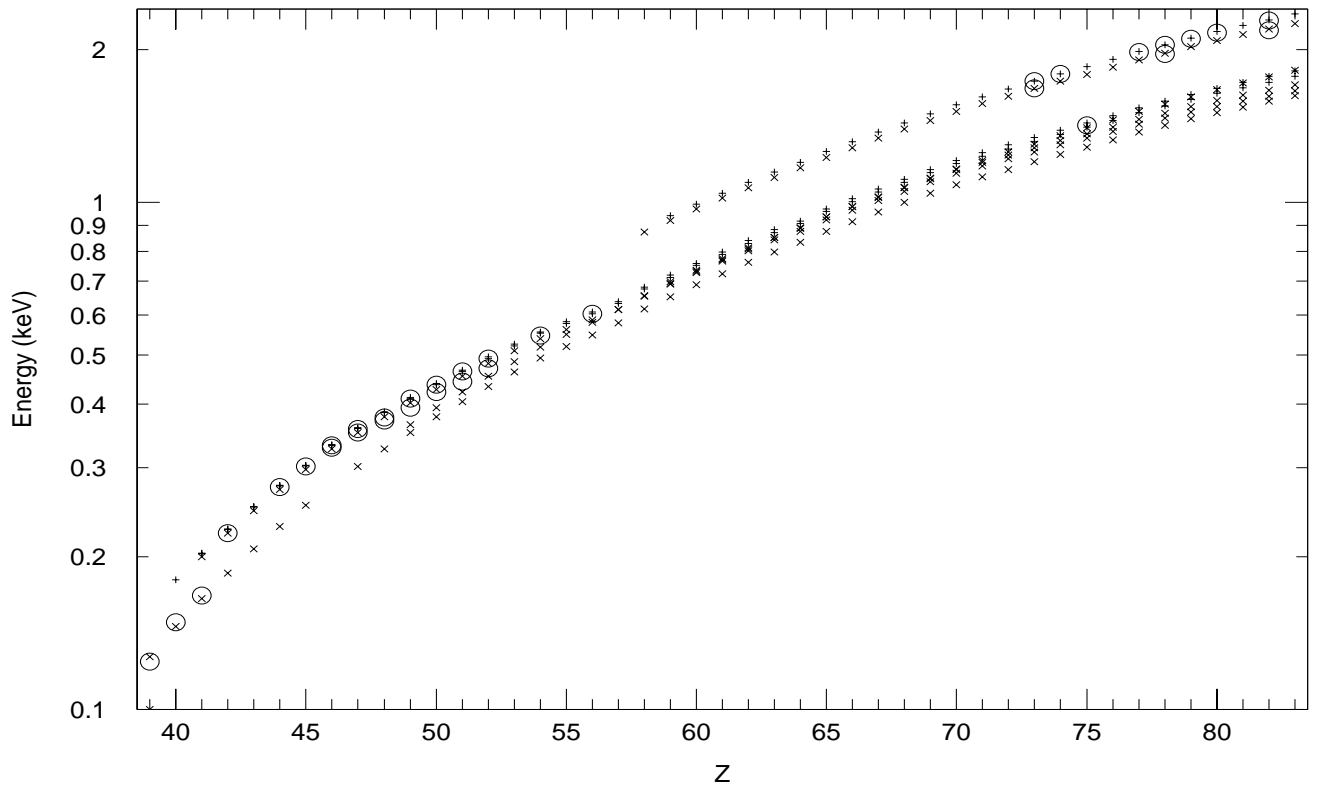


Fig. 10. Auger electron energies resulting from Geant4 M₄ (“+”) and M₅ (“x”) transitions and NIST reference experimental data (open circles); to improve the readability of the plot the symbols representing NIST data are scaled by a factor 2 in size with respect to the symbols representing Geant4 simulation.

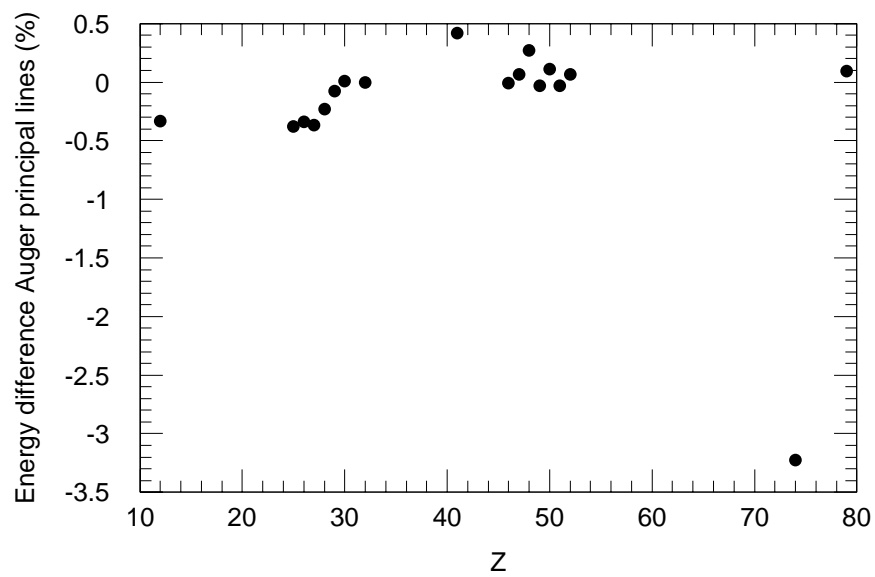


Fig. 11. Difference between Geant4-simulated and NIST reference electron energies for Auger principal lines as a function of the atomic number Z ; they are expressed in percentage with respect to the NIST value.